S5-011

Structural studies of cyanobacterial photosystem II

PCA da Fonseca, EP Morris, J Barber

Wolfson Laboratories, Department of Biological Sciences, Imperial College of Science, Technology and Medicine, London SW7 2AY, UK

Keywords: cyanobacterial PSII, structure, electron crystallography, two-dimensional crystals

Introduction

The determination of the structure of PSII at high resolution is required in order to fully understand its unique reaction mechanisms. The information so far available on the structure of the transmembrane domain of the higher plant PSII core dimer complex has been obtained by cryo-electron crystallography of the spinach CP47-PSII reaction centre (CP47-RC) subcomplex, yielding a three-dimensional (3D) map at a resolution of 8 Å (Rhee, 1998; Rhee *et al*., 1998), and of the spinach PSII core dimer for which a 9 Å projection map was initially calculated (Hankamer *et al*., 1999) and subsequently a 10 Å 3D map was elucidated (Hankamer *et al*., 2001). From the analyses of these maps it was possible to identify densities corresponding to the transmembrane α-helices of the D1, D2, CP43, CP47 and cyt b559. In addition a further ten α-helices were identified in each monomer of the core dimer complex corresponding to still unassigned low molecular weight subunits (Hankamer *et al*., 2001).

The resolution of the structural data obtained on higher plant PSII complexes has been limited by the size and order of the 2D crystals analysed. For this reason PSII core complexes have been isolated from the thermophilic cyanobacterium *S. elongatus* and used to produce two-dimensional (2D) crystals. This cyanobacterium grows at temperatures above 55°C and it has been shown that PSII core complexes derived from this source are more active and stable than the PSII complexes prepared from higher plants (Schatz and Witt, 1984). Indeed, they have proven to be suitable for growing 3D crystals of PSII for x-ray diffraction analysis and as a result a 3D structural model of PSII at 3.8 Å resolution has recently been published (Zouni *et al*., 2001). Here the structural data on the cyanobacterial PSII obtained by electron crystallography and x-ray analysis are compared with the data available on the spinach PSII core dimer.

Materials and methods

S. elongatus PSII core dimers were purified and characterised as previously described (Nield *et al*., 2000) and 2D crystals were produced by *in vitro* reconstitution. All crystallisation trials were conducted using freshly purified PSII complexes, since it was found that the quantity and quality of the crystalline areas severely decreased when the samples used had been previously frozen. During the optimisation of the 2D crystallisation conditions each trial was evaluated and recorded by electron microscopy of negative stained samples on a Philips CM100 electron microscope. When the quantity and quality of the crystalline regions was observed to be high they were recorded by cryo-electron microscopy on a Philips CM200-FEG microscope, under low-dose conditions. All electron microscope grids were glow discharged prior to the sample application in order to increase the flatness of the crystalline areas. The micrographs selected for image processing were digitised using a patch

densitometer (Schatz *et al*., 1994). Image processing was performed using the MRC suite of programs (Crowther *et al*., 1996) together with locally developed software.

Results and discussion

Projection map of the Synechococcus elongatus PSII dimer complex

The projection map obtained from the image processing of the *S. elongatus* PSII dimer 2D crystals, at a resolution of approximately 16 Å, is presented in Fig. 1. The crystal sheets obtained belong to the two-sided plane group $p22_12_1$ and the unit cell parameters are a=121Å, b=333Å and $\alpha=90^o$. One important feature of the $p22_12_1$ plane group is its set of in-plane screw axes. These screw axes arise from the PSII complexes being inserted into the reconstituted lipid membrane in two opposite orientations, so that a projection map shows both lumenal and stromal views of the complex which are mirror images of each other. A significant advantage of 2D crystals with this plane group symmetry is that theoretically such crystal sheets can grow indefinitely and are intrinsically flat. In contrast, 2D crystals in which all molecules have the same polarity, such as the ones previously obtained for spinach PSII core complexes (Morris *et al*., 1997, Hankamer *et al*., 1999) usually have a tendency to form curved sheets, which places a limit on the size and order of such crystals.

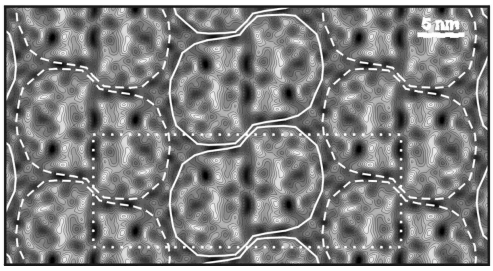

Fig. 1 - Projection map determined by image processing of 2D crystals of *S. elongatus* PSII core dimers. One of the unit cells is outlined (dotted line). These crystals belong to the two-sided plane group $p22_12_1$ and as a result the projection map shows both lumenal (continuous outline) and stromal (dashed outline) views of the complex, which are mirror images of each other.

Comparison of the structural data on the Synechococcus elongatus PSII core dimer obtained by electron crystallography and x-ray analysis

The transmembrane domain (Fig. 2B) and the complete 3D model (Fig 2A) of the *S. elongatus* core dimer obtained by x-ray crystallography at 3.8Å (Zouni *et al*., 2001) is overlaid onto our 2D projection map derived from the same complex. Although the latter is at a resolution of 16Å there is considerable agreement between the electron crystallographic data and the transmembrane domain of the 3D model derived from x-ray analysis (Fig. 2A). The projection map also clearly shows the density that corresponds to the β-strand cylindrical domain (indicated by white arrows in Fig. 2) assigned in the 3D model to a part of the extrinsic 33 kDa PsbO manganese stabilising protein. The agreement between the 3.8Å x-ray derived 3D model and the densities within our projection map clearly indicate the reliability of the data obtained by electron crystallography.

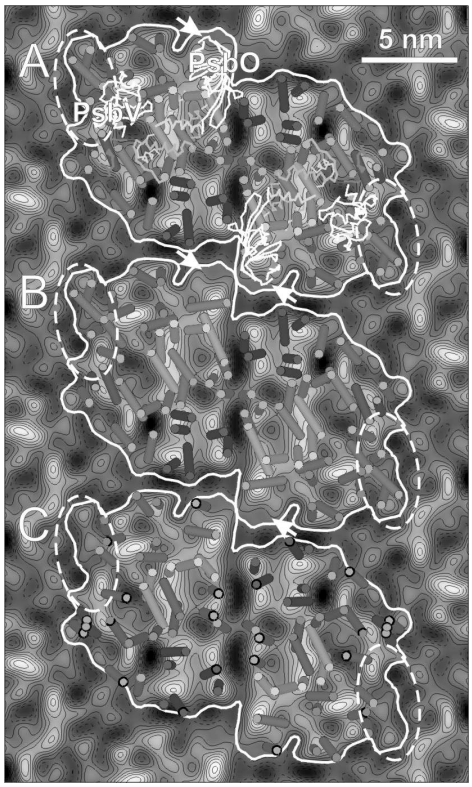

Fig. 2 - Comparison of the *S. elongatus* PSII core 16 Å projection map with structural models of PSII. The projection map is overlaid with: **A** - the full 3D model of *S. elongatus* derived from x-ray crystallography (Zouni et al., 2001); **B** - the transmembrane helices of the model presented in **A**; **C** - the transmembrane helices of the spinach core dimer deduced from electron crystallography (Hankamer et al., 2001). The *S. elongatus* core dimer is outlined in white. In each monomer the region corresponding to the main differences between the cyanobacterial and spinach models is outlined by a dashed line. The arrows identify the protein density corresponding to a domain of the PsbO extrinsic protein.

Comparison of the structural data on Synechococcus elongatus and spinach PSII core dimer complexes and its biological relevance

The membrane spanning subunits of PSII are highly conserved between higher plants and cyanobacteria which suggests a similar organisation of their transmembrane domains. Here we compare our projection map of *S. elongatus* PSII with the 9Å projection map previously obtained by electron crystallographic analyses of the spinach PSII core dimer complex (Hankamer *et al*., 1999). This comparison (shown in Fig. 3) emphasises that the PSII complex of higher plants and cyanobacteria are dimeric. Overall they share similar density distribution but there are some differences. In particular the spinach projection map has a lower level of density in the region ringed with a dashed line in Fig. 3.

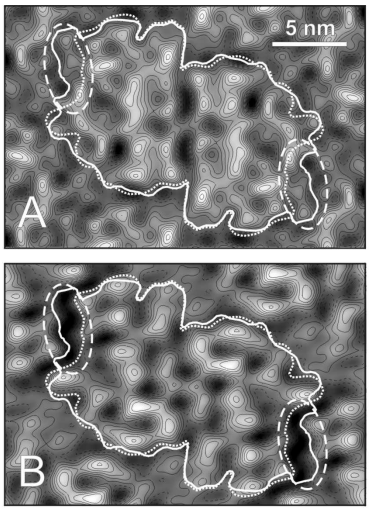

Fig 3 - Comparison of the *S. elongatus* (**A**) and spinach (**B**) PSII core projection maps. The data in **B** were derived from (Hankamer *et al.*, 1999). In both panels the outline of the *S. elongatus* core dimer is identified by continuous white lines, while the outline of the spinach complex is represented as a dotted lines. The dashed ellipses in **A** and **B** identify the main differences between the two projection maps.

In order to gain a better understanding of the differences between the projection maps of *S. elongatus* and spinach, the 3D model of the transmembrane helices of the spinach PSII core complex obtained by electron crystallography (Hankamer *et al*., 2001) is overlaid onto our *S. elongatus* projection map (Fig. 2C) and are compared with the helices from the *S. elongatus* PSII 3D model obtained by x-ray crystallography (Fig. 2B). In both 3D models the relative positioning of the transmembrane helices of the main subunits, D1, D2, CP43, CP47 and cyt b559, is essentially identical within each monomer. These subunits are related to each other in the same way within the dimers, emphasising the conservation of the basic structural features of PSII between higher plants and cyanobacteria. The positioning of many of the transmembrane helices of the low molecular weight subunits is also conserved between the two systems. However the dissimilarity identified in Fig. 3 is related to a lack of a cluster of four transmembrane helices close to helices 1 and 2 of CP43 in the spinach structure, compared with that of *S. elongatus* (dashed outline in Fig. 2). These differences in the content and location of small subunits appear to reflect variations in the PSII complex between spinach and *S. elongatus* although it is also possible that they may be related to the differential retention of particular small subunits during the preparation procedures.

Variations in the small subunits adjacent to the CP43 subunit may be related to functional adaptations. In *S. elongatus* this region is close to the extrinsic PsbV subunit. Higher plants do not have this extrinsic cytochrome and instead bind distinctly different extrinsic proteins. Moreover, cyanobacterial PSII interacts with phycobilisomes bound to the stromal surface of thylakoid membrane, instead of the intrinsic outer light-harvesting complex of higher plants. Given these distinct features between higher plant and cyanobacterial systems it seems reasonable that there could be some differences within the transmembrane regions of the PSII core dimers of the two classes of organisms. Also to be noted is that *S. elongatus* is a thermophile while spinach is not, a factor that may also be related to the observed differences.

Acknowledgements

We wish to thank the Biotechnology and Biological Sciences Research Council (BBSRC) for financial support. Paula da Fonseca was supported on the PRAXIS XXI program.

References

Crowther RA, Henderson R, Smith JM (1996) *Journal of Structural Biology* **116**, 9-16.

Hankamer B, Morris EP, Barber J (1999) *Nature Structural Biology* **6**, 560-564.

Hankamer B, Morris EP, Gerle C, Nield J, Barber J (2001) *Journal of Structural Biology* in press.

Morris EP, Hankamer B, Zheleva D, Friso G, Barber J (1997) *Structure* **5,** 837-849.

Nield J, Kruse O, Ruprecht J, da Fonseca P, Büchel C, Barber (2000) *Journal of Biological Chemistry* **36**, 27940-27946.

Rhee KH (1998) Ph.D. Thesis, University of Heidelberg, Germany.

Rhee KH, Morris EP, Barber J, Kühlbrandt W (1998) *Nature* **396**, 283-286.

Schatz GH, Witt HT (1984) *Photobiochemistry Photobiophysics* **7**, 1-14.

Schatz M, Zeitler E, van Heel M, (1994) International Conference on Electron Microscopy – 13, 425-426.

Zouni A, Witt HT, Kern J, Fromme P, Krauβ N, Saenger W, Jordan R, Orth P (2001) *Nature* **409**, 739-743.